Novel R2R Manufacturable Photonic-Enhanced Thin Film Solar Cells

January 28, 2010 — January 31, 2011

Dennis Slafer
Lightwave Power
Cambridge, Massachusetts

Vikram Dalal
Iowa State University
Ames, Iowa

NREL

NATIONAL RENEWABLE ENERGY LABORATORY

Novel R2R Manufacturable Photonic-Enhanced Thin Film Solar Cells

January 28, 2010 — January 31, 2011

Dennis Slafer
Lightwave Power
Cambridge, Massachusetts

Vikram Dalal
Iowa State University
Ames, Iowa

NREL is a national laboratory of the U.S. Department of Energy, Office of Energy Efficiency & Renewable Energy, operated by the Alliance for Sustainable Energy, LLC.

This publication received minimal editorial review at NREL.

Table of Contents

1 SUMMARY

1.1   Overall Program Results

The goal of this program was to produce tandem Si cells using photonic bandgap enhancement technology developed at ISU and Lightwave Power that would have an NREL-verified efficiency of 7.5% on 0.25 cm2 area tandem junction cell on plastic substrates. This goal was met and exceeded within the timeframe and budget of the program. On smaller area cells, the efficiency was even higher, ~9.5% (not verified by NREL). Appropriate polymers were developed to fabricate photonic and plasmonic devices on stainless steel, Kapton and PEN substrates. A novel photonic-plasmon structure was developed which shows a promise of improving light absorption in thin film cells, a better light absorption than by any other scheme. Various aspects of this work have also been included in a paper in Appendix D.

1.1.1   Summary of Results by Quarter: Q1

The work carried out during the first quarterly reporting period, 28 January, 2010 to 27 April, 2010 included the design of the Photonic Band Gap (PBG) nanostructure for enhanced light trapping at the back of the PV cell, the fabrication of soft and hard tooling required to replicate the PBG structure, and production of flexible polymeric substrates having this structure, and the initial depositions of a-Si PV layers on PBG films. Contract Deliverable #1 was also successfully completed in Q1.

1.1.2   Summary of Results: Q2

During the second quarterly reporting period, 28 April 2010 through 27 July 2010, the principal technical efforts included the formation and optimization of flexible substrates having the PBG nanostructure using the soft and hard tooling that was described in the previous Report. A number of a-Si PV devices were fabricated using the PBG substrate. Contract Deliverable #2 ("Intermediate/Due 7/28") was also successfully completed in this reporting period and delivered 2 months early (NREL Test Results for 5/17/10, appended).

1.1.3   Summary of Results: Q3

During the third quarterly reporting period, 28 July 2010 through 27 October 2010, technical efforts included fabrication of tandem junction solar cells and continued improvement of the nanoimprint process for forming flexible substrates having a PBG-enhanced substrate.

1.1.4   Summary of Results: Q4

For the fourth and final quarter of the program, running from 28 October 2010 through 31 January 2011, the main technical focus was the fabrication of tandem junction cells on a PBG polymer substrate. Tandem junction solar cells, measured at NREL, showed an efficiency of ~7.6%, exceeding the target of 7.5%. Small area cells, measured at Iowa State but not at NREL, had even higher efficiency, between 8.5 and 9.0%.

Unless otherwise noted, all images in this work are property of the authors.

2 INTRODUCTION

2.1 Background

Photovoltaic energy conversion is a rapidly growing industry that amounted to about 2.8 GW of production in 2007, and has grown at an annual growth rate of approximately 40% over the last 5 years [1]. It is now producing electricity at ~20c/kWh [2]. To be cost-competitive, the levelized cost of electricity (LCOE) produced has to be below 10 c/kWh. The current PV industry is based about 90% on crystalline Si technology, using Si wafers. The remaining 10% is thin films, divided between thin film Si (both amorphous and microcrystalline or nano Si), CdTe and CIGS. Because of the high cost of Si wafers, the thin film market segment is growing very rapidly, with many industries having announced GW size manufacturing plants, including for both amorphous Si (a-Si) and nanocrystalline thin film Silicon (nc-Si)[3-5].

However, it is very clear that to achieve low cost LCOE, it is necessary to have both low cost and reasonable conversion efficiency. The present day a-Si based modules are only in the 8-9% range, and this lower efficiency has a detrimental impact on LCOE because the area related costs become too high. Nano Si panels with a tandem cell module based on amorphous/nano Si cell design exhibit efficiencies in the 10% range. To achieve lower LCOE, one has to increase efficiencies of thin film modules to the same range as efficiency of multi-crystalline Si modules, namely15%. To do this, it will be necessary to increase conversion efficiencies of tandem junction cells based on thin-film Si to 19-20% range from the present 15% [6]. This will require major changes in cell designs and architecture. Our project proposes a revolutionary new design that can achieve such higher efficiencies in the future.

One of the major disadvantages of any thin film Si technology is that the material has to be thin. In nano Si, the diffusion length is of the order of a few micrometers [7], which forces the thickness of the i layer in a p-i-n cell in nano Si to be of the order of 1-2 micrometer. Since Si is an indirect bandgap material, such a thin layer does not allow for efficient photon absorption. Therefore, one needs to enhance light absorption in the material. One way to do this is to use texturing leading to light trapping [8]. A popular texturing method is to use textured silver back reflector [9] followed by a ZnO layer, the combination of which increases light trapping. However, surface plasmons generated in textured silver limits this scheme to a factor of ~5 optical enhancement. To overcome this, we suggest a very novel scheme. The strategy is to use a photonic bandgap (PBG) as the back reflector (see Fig. 1 for a schematic diagram of the periodic PBG structure that we have invented). It consists of a periodic array of a conducting material such as ZnO, which acts as a 2 dimensional PBG diffraction grating, forcing incoming light to bend sideways. This light is totally internally reflected at the top surface, thereby creating light trapping and multiple light absorption. Computer simulations [10] indicate that such a PBG structure can enhance absorption by about a factor of 20 (see Fig.2). The factor of 20 is far higher than a factor of 4-5 that is typical of textured Ag.

To make such a structure, we have invented a new method--nano-imprinted plastic substrates coated with a thin layer of silver followed by ZnO (see Fig. 3 for our new device geometry). *The precisely formed nano-imprinted structure, coated with Ag/ZnO, act as a photonic bandgap.* Note that our structure is revolutionary, in that we plan to use roll-to-roll (R2R) *nano-imprinting technology on plastic substrates*, a very different scheme from the normal way of making PBG structures which

relies on very high cost optical or e-beam lithography (see Fig. 4 for SEM of one of our PBG arrays etched into Si). We also plan to use a very low cost plastic substrate to deposit our nano-Si cell. Other approaches use a very expensive Kapton (polyimide) substrate, which limits its general applicability. In contrast, the goal of this program is to use PEN, which is a much lower cost substrate, and capable of reaching a ~230 °C working temperature. PEN can also easily support nano-imprinting. Thus, our eventual objective is to produce stable, high efficiency (19-20%) tandem junction cells based on a-Si/nano Si combination on low cost plastic substrates using an inexpensive roll-to-roll manufacturing technique.
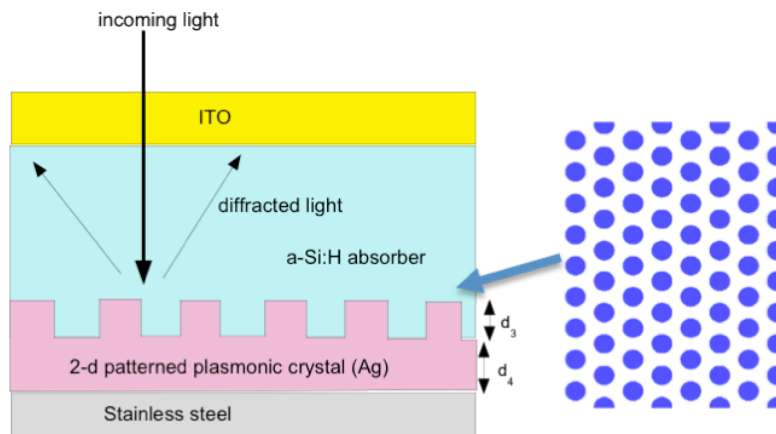

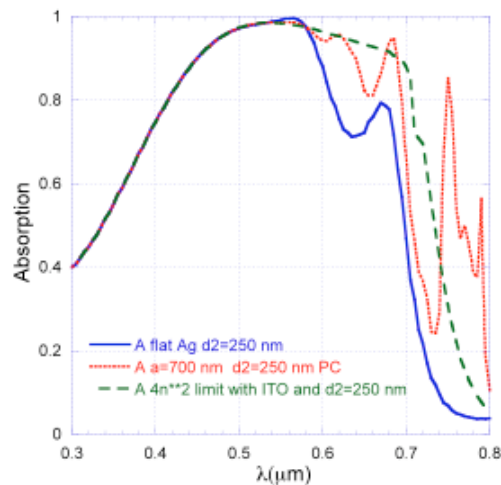**Fig 1. A photonic array for efficient back reflection**

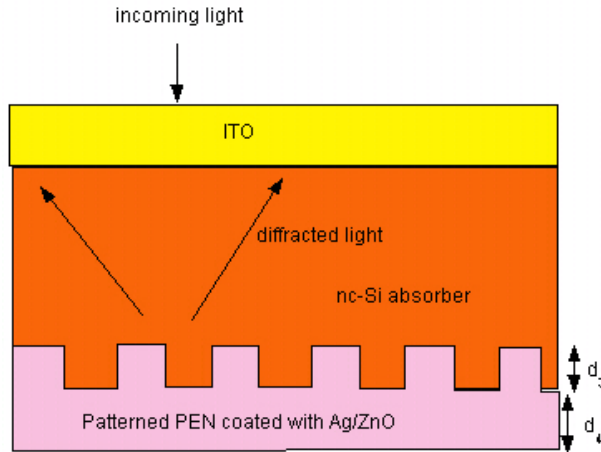**Fig 2. Calculated enhancement in light absorption (blue curve) using photonic reflector**

3

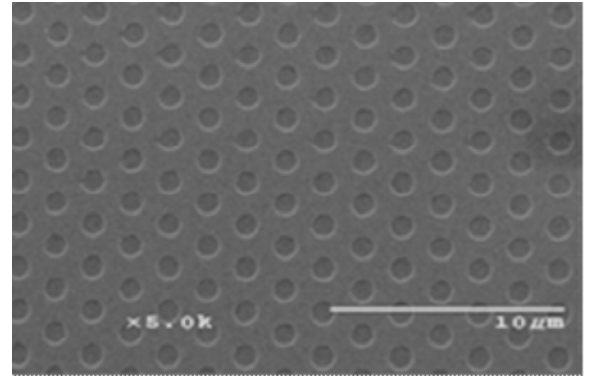**Fig 3.** Our new proposed photonic PBG array on PEN

Fig 4. SEM of A photonic reflector array etched into Si wafers at Iowa State

2.1.1 Scattering Matrix Simulations

Summary

- Maxwell's equations were solved in Fourier space

- **E, H** fields were expanded in plane waves

- Both polarizations of the incident wave were calculated

- Structure (e.g. Solar cell) was divided into layers

- Within each layer, reflection and transmission were calculated

- All layers were put together and the reflection, transmission and absorption of the entire structure was calculated

- Fully parallelized– each frequency was sent to a different processor

The advantages of this approach over real space methods in that it can deal with very thick substrates and large variations of E, H fields. Another advantage is that it can analyze any number of layers, each with its own n and k values. The details of this work have been presented in several papers [11-13] and the interested reader is referred to these papers for details.

2.1.2 Fabrication of Nano Array Substrate

In order to form the photonic nanostructures required to trap incident light, a novel technology for producing such patterns in on polymeric substrates was used. This technology, called Advanced Surface Nanoforming (ASN), is capable of molding nano-array patterns on flexible films by a roll-to-roll process. In this process, a master template is formed using 3-beam laser interferometry [14] to form a 3-axis standing wave interference pattern onto the surface of a photoresist-coated substrate, and development of the photoresist produces a hexagonal array of cells/pillars. This interference technique is capable of forming such patterns over large areas in a single exposure.

Control of the beam convergence angles and exposure/development conditions allows adjustment of the pitch and duty-cycle of the interference pattern (constructive and destructive optical field), shown schematically in Fig. 5.
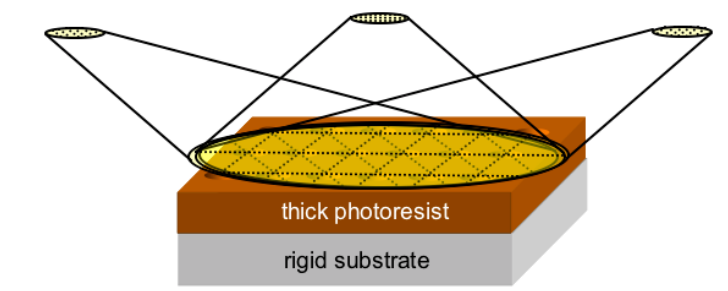

Fig 5. Use of multibeam laser interferometry to produce photonic array master pattern in a single exposure. 3-D pattern is formed after development of exposed photoresist

In order to form the photonic nanostructures over very large areas and inexpensively, a novel technology for producing such patterns in on polymeric substrates was used. This technology, called Advanced Surface Nanoforming (ASN), was developed for molding nano-array patterns on flexible films by a roll-to-roll process. Direct-write techniques, such as e-beam lithography, are used to form a *single* master template having the desired 3-D nano photo-plasmonic structures. The master template can be positive or negative (bumps or depressions), as the multi-generational replication process is capable of producing interchanged structures. For typical substrates, the ASN process uses precision Ni electroforming to create a family of nanoimprinting tools that are used to replicate the photonic pattern (see Fig. 6).

Although outside the scope of this program, the process is designed for ultimate use in R2R manufacturing. Here, the Ni tool is formed into a cylinder, similar to that used in the graphic arts flexographic printing process and allows high-precision imprinting of radiation cured layers on flexible plastic and metal foil substrates. In this process, the rotary imprinting tool itself is transparent and uses a new, solid-state radiation source to crosslink a liquid patterning polymer. This transparent rotary tool is used to continuously form the photo-plasmonic layer in a single unwind-to-rewind pass, which is followed by a subsequent pass in a R2R vacuum coater in which the conductive/reflective layers are deposited. This material will serve as the foundation substrate for the next steps, deposition of the tandem PV layers. The key R2R nanopatterning step is illustrated in the schematic in Fig. 7a, which shows an unwind station for feeding the carrier substrate into the pattern forming station, an in-line laser-based diffraction measurement station, and a rewind station for the patterned substrate. A photograph of an ASN pilot process machine is given in Fig. 7b. Fig. 8 shows the schematic of a R2R machine for sputtering the metal and ZnO layers, and Fig. 9 shows various photographs of the R2R type imprinter.

These pilot processors have already been used to produce many thousands of feet of various nanopatterned substrates at a production rate of many square feet per minute, a process which would otherwise take many hours *per square inch* if direct write (e-beam, etc.) were required to form each pattern.
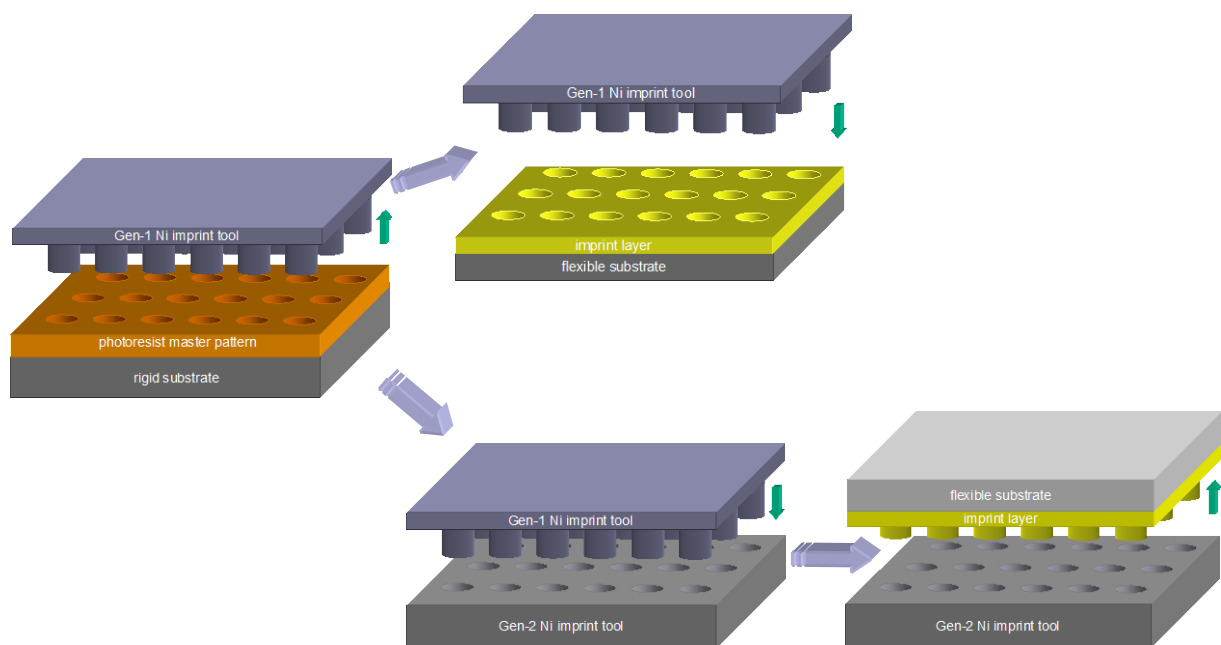
Fig 6. Process steps for forming durable manufacturing tooling and for imprinting photonic array on flexible substrate. Ni tool is electroformed from master pattern (left) and used to replicate pattern on flexible substrate (right)
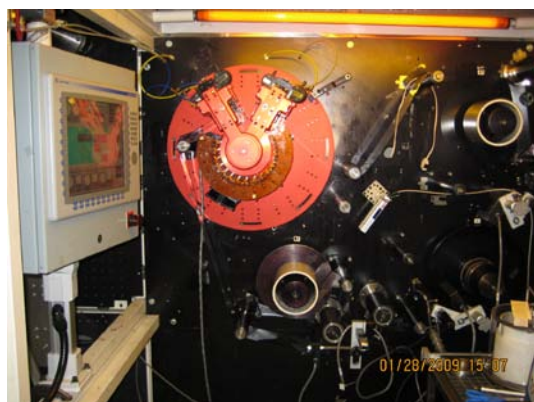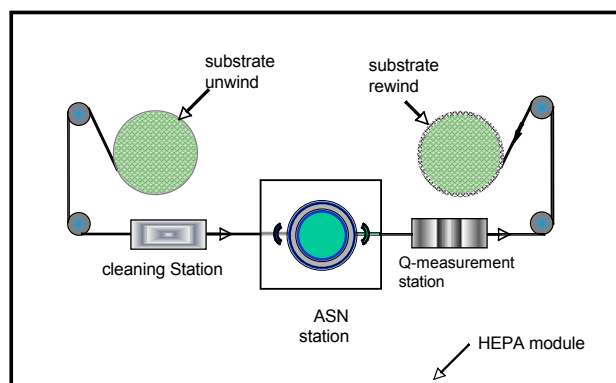

Fig 7 (a, b). Schematic of ASN process for replicating photonic array (l), consisting of a substrate unwind station, film pre-cleaner, nanoimprint station, Q-measurement station, and rewind. Photograph on right shows the imprint station of a pilot R 2R imprint machine designed for processing 150mm wide substrates.
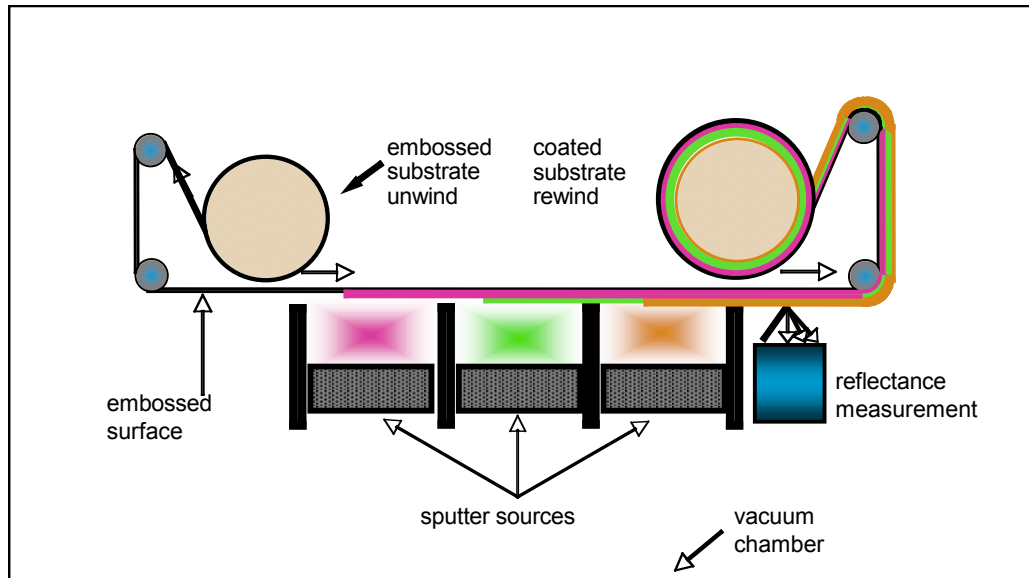
6

Fig 8. R2R sputter coater used to deposit conductive and/or reflective layers on patterned substrate. Rolls of material made in the imprinter (Figs 2, 4) are unwound from left station so that the patterned surface faces down when traversing the deposition zones (i.e., no face-side contact to damage the nanopattern), then rewound onto right spool. Reflectivity can be measured after deposition zone(s) to control layer uniformity.
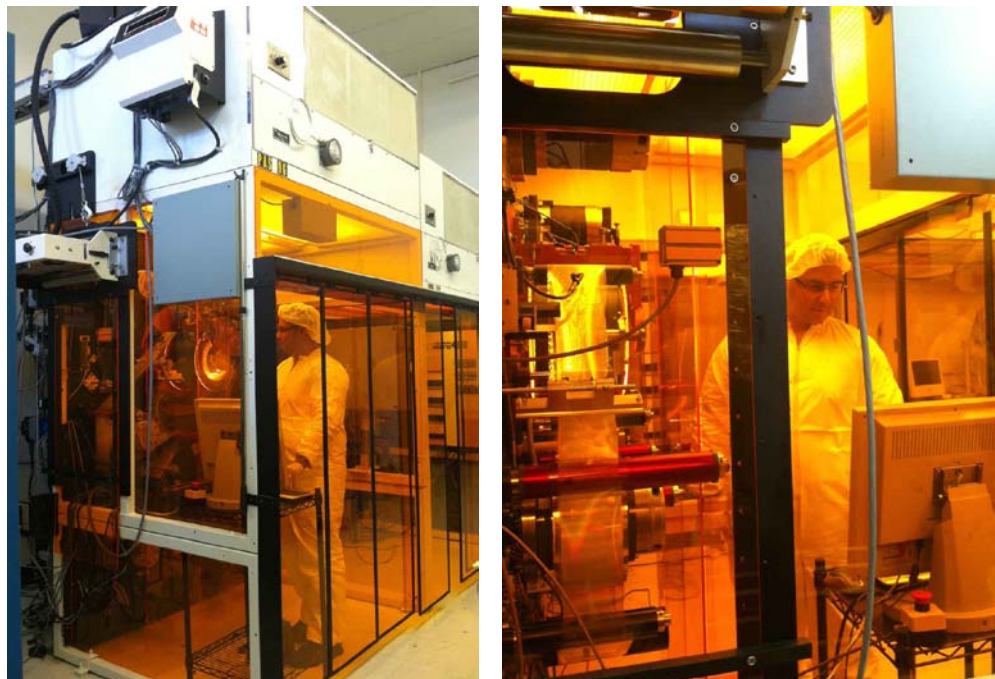

Fig 9. External views of MOD3 ASN processor/HEPA module (l, center); vacuum roll coater (r) with four in-line sputter cathodes (RF & DC magnetron) for depositing metallic and dielectric layers.
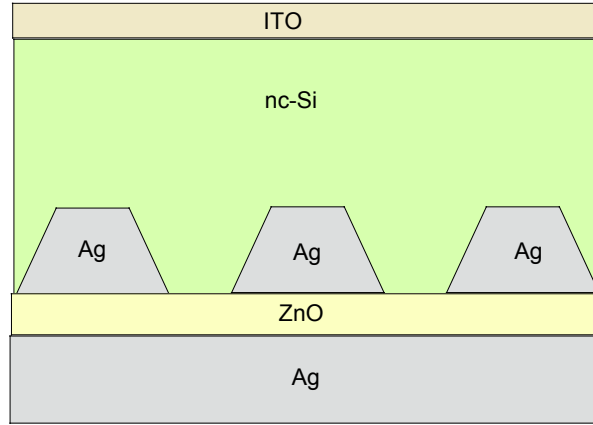
Fig 10. Photo-plasmonic structure for enhancing light absorption. The structure is imprinted into a polymer that is coated on top of a steel substrate.

2.1.3 Fabrication of solar cell devices

<u>Fabrication procedure for a-Si devices on photonic plasmon substrates</u>
The nano-imprinted substrates received from Lightwave Power have the photonic plasmon structure on them. They are cleaned in methanol and dried and then Ag is evaporated on them to a thickness of 200 nm in a thermal evaporator. Then, a 100 nm layer of Al doped ZnO is sputtered on the Ag coated photonic plasmon using a RF sputtering system and Ar as the sputter gas. The target is ZnO doped 1% with Al. Before depositing on the substrate, the target is cleaned for 2 minutes in an Ar plasma and then the shutter which isolates the substrate from the target is opened and ZnO:Al sputtered on Ag coated photonic plasmon. During the sputtering process, the pressure is maintained at   5 mTorr, the substrate temperature at 200 C, and the RF power at 75 W.

After sputtering of ZnO, the substrate is loaded into a VHF PECVD reacto*r* for depositing the p-i-n a-Si:H cell. The VHF frequency is ~45 MHz. First, a n+ a(Si,C):H layer is deposited on the sample from mixtures of silane, methane, hydrogen and phosphine. The objective behind using a-(Si,C):H is to minimize absorption losses in the n+ layer, and allow reflected photons to traverse this layer with minimum absorption. Typical deposition conditions are to use T=250 C for the substrate and pressure of 50-100 mT. After depositing the n+ layer, the gases are evacuated and the chamber is purged 10 times with nitrogen to exhaust any residual phosphine. Then the chamber is purged with silane and hydrogen many times, and finally, a 15 minute plasma cleaning procedure is used to overcoat any n+ layers on the chamber walls[15]. During this procedure, the sample is covered with a shutter so as to prevent any deposition on it. After such a cleaning, the active I layer is deposited, followed by a very thin a-(Si,C) graded gap buffer layer [16] so as to prevent recombination of electron-hole pairs at the p-i interface. Finally, the top p+ layer is deposited using mixtures of silane, hydrogen, methane and diborane. The substrate temperature during the growth of the p layer is lower, about 200 C. The p layer is followed by the sputtering of 75 nm of ITO at a temperature of 150C. During this sputtering, the Ar gas is mixed with small amounts of oxygen so as to achieve the correct stoichiometry for ITO. Fig. 11 shows the typical optical absorption characteristics of the ITO layer. A thicker ITO layer is used for this measurement as compared to the thin ITO layer used

for devices. The thickness of the ITO layer for devices is based on achieving an optimum anti-reflection effect. A photograph of the reactor used for depositing a-Si is shown in Fig. 12.
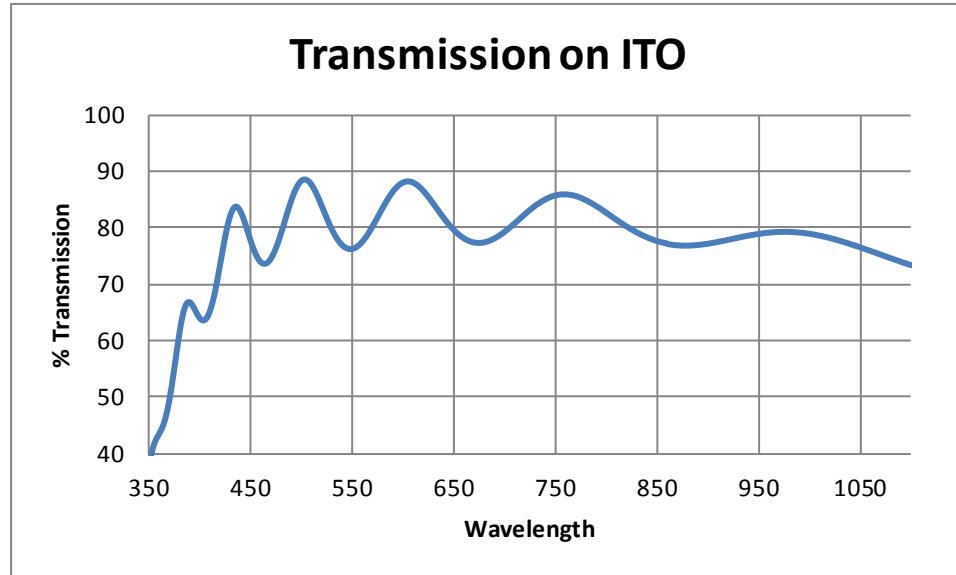

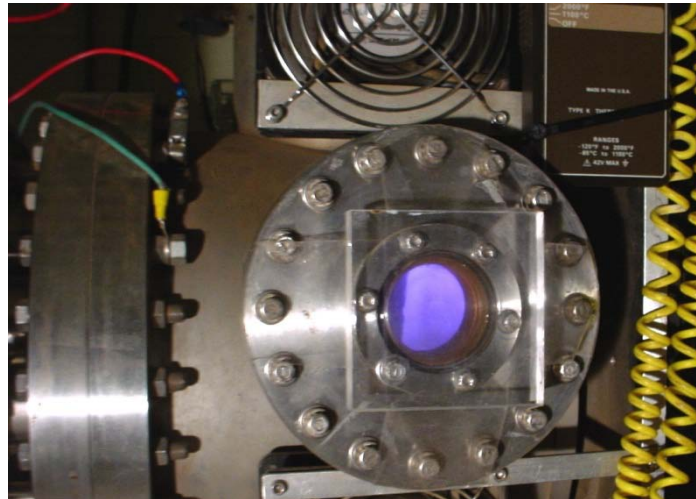**Fig 11. Transmission data for a thick ITO film**

Fig 12. Plasma reactor used for depositing a-Si top cell

Fabrication procedure for tandem junction a-Si/nano Si solar cells on photonic plasmon substrates

The tandem junction a-Si/nano Si solar cells are fabricated on photonic plasmon structures nano-imprinted into Kapton substrates. The substrates are coated with 200nm of Ag and 100 nm of ZnO as described above. After the deposition of ZnO, the substrates are moved to the reactor for depositing nano Si. It is a diode coupled VHF PECVD reactor capable of having layers deposited at frequencies ranging from a few MHz to 50 MHz. An Agilent signal generator is coupled into an

ENI power amplifier that provides the power to the reactor. Typical frequencies that we use are ~45 MHz. The typical growth temperatures for growing nano Si cells on the photonic plasmon substrates are ~225 C and pressure is 100mT. The i layer of the p-i-n cell cells was grown using a graded hydrogen:silane dilution ratio which varied during growth, decreasing from 3);1 at the initiation of the crystalline layer to about 15:1 at the end[17]. After the i layer deposition, a p+ nano Si layer was deposited from mixtures of silane, hydrogen and diborane, using VHF PECVD, again at 45 MHz frequency.

Next, the top p-i-n a-Si cell was deposited, starting with the n+ layer. Next, an appropriate thickness of the amorphous Si i layer was deposited as described in paragraph 1 above. The thickness was calculated using optical constants of a-Si and nano Si so that the currents in the top and bottom cells could be matched. The I layer was followed by the buffer layer and the p+ a-Si layer as described above. Finally, a 75 nm ITO layer was deposited to make the ohmic contact, as described in paragraph 1 above.

In Fig. 13, we show the I-V curve of a small area cell, ~0.105cm^2, deposited on Kapton, with an efficiency of ~9.5% (not verified by NREL). Note the excellent fill factor, signifying very good properties for the p+/n+ tunnel junction, which connects the two cells. In Fig. 14, we show the corresponding quantum efficiency curves for each of the component cells showing the excellent agreement between currents produced in the top and the bottom cells.
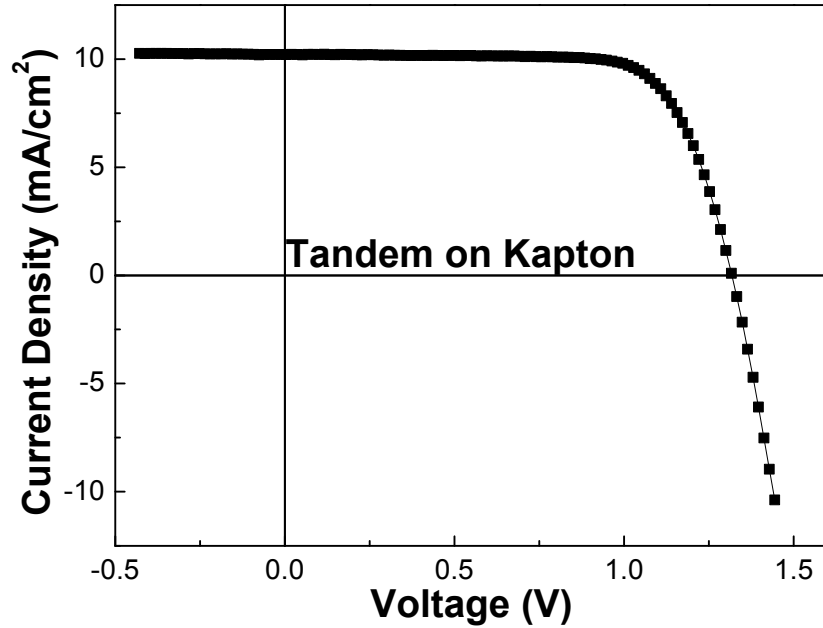

Fig 13. I-V curve of small area a-Si/nano Si tandem junction solar cell on Kapton substrate.
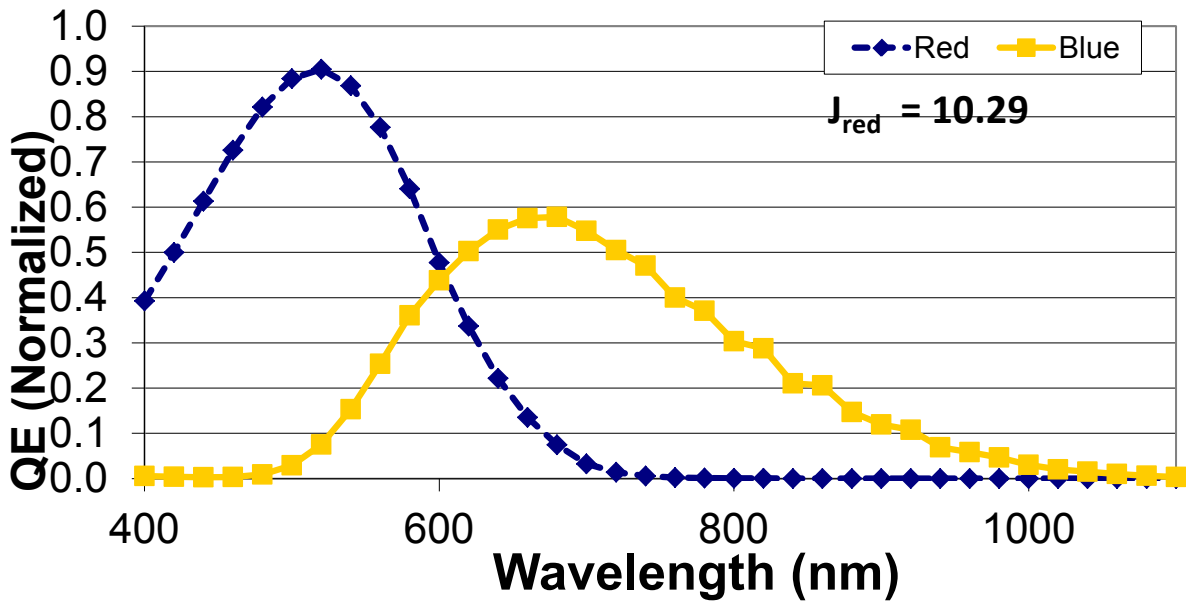
Fig 14.   QE curves for top and bottom cells measured using red light bias (top cell) and blue light bias (bottom cell).

Several papers have been published on device fabrication and results [18-20], and the interested reader is referred to these papers.

3   OBJECTIVES

The primary <u>Technical Improvement Opportunities</u> (TIO) for this project were:
1. To significantly improve light absorption in nano Si and thereby increase efficiency
2. Use a low cost plastic substrate and production-type photonic technology to reduce LCOE

The primary program objectives were:

1. To design and fabricate optimized nano-imprinted photonic bandgap light enhancement structures and study their optical properties with thin film of nano Si deposited on them.

2. To fabricate working solar cells on PEN substrates with the photonic structure with reasonable efficiencies in this first phase. For comparison, photonic bandgap PEN coated with Ag/ZnO will be evaluated against plain PEN coated with Ag/ZnO (control cell). A study of the quantum efficiency (QE) of the two cells will reveal how additional light absorption is achieved by our experimental cell. By achieving these objectives in this incubator phase, we can proceed to make efficient and stable tandem junction thin film Si based cells and modules in future projects.

3.1   Tasks and Results
The program began with a photonic band gap structure being generated by computer model. Using the model structure as input, the design was converted into a direct write tool path in a

semiconductor fab and reproduced in etched silicon (sketch of the mastering and replication process was previously shown in Fig. 6, and SEM of actual patterns are shown in Figs 15-16). Multiple-beam laser interferometry was also used to make master patterns, but the higher uniformity produced by the direct write process combined with its shorter 'learning curve' resulted in its selection as the preferred method for tooling generation within the constrains of the present program. We feel, however, that further development of the laser approach will ultimately provide a better approach for making very large-area nanopatterns.

The silicon master formed by the direct write process was used to produce several sets of soft and hard tools (described previously, Sec 2.1.2) that in turn were used to produce the nanopatterned flexible substrates upon which the a-Si cells were built. It should be noted that only a single--although very expensive--master silicon pattern was required for the entire program, and all of the subsequent soft and hard tool generations required for this program came from this single master. Since the master pattern was used only to form the working tools, this approach eliminated the concern of damaging or otherwise contaminating the Si master by using it for direct imprinting. The imprint tools used to produce the polymer replicas, on the other hand, were very inexpensive and could be replaced readily. Generation 1 and Generation 2 tools ("negatives" and "positives") were both formed (in sequence) from the original master pattern, thus both bumps and holes could be formed through our process. With the peak-to-valley wavelength phase shift being essentially equivalent for both structures, both were evaluated during the program. The bump geometry was ultimately preferred over the hole geometry due to the former's gentler sloping topography at the base of the structure that helped to eliminate the sharp angles that contributed to electrical layer shorting.

The Gen-1 and Gen-2 tooling was used to form the PBG structure in various types of flexible polymer and foil films, including PET, Kapton, stainless steel and the preferred substrate, PEN. Numerous samples were produced with PBG-patterned areas of up to 3.5 x 3.5-in. Samples of these materials were analyzed using SEM and diffraction measurements to confirm the structure. SEMs of the master pattern in etched silicon are shown in Figs. 15 and 16, and polymer replicas made from tooling from this master pattern are given in Fig. 17. The completed design served as **Deliverable #1 (Baseline Deliverable)** for the program, which was completed on schedule.
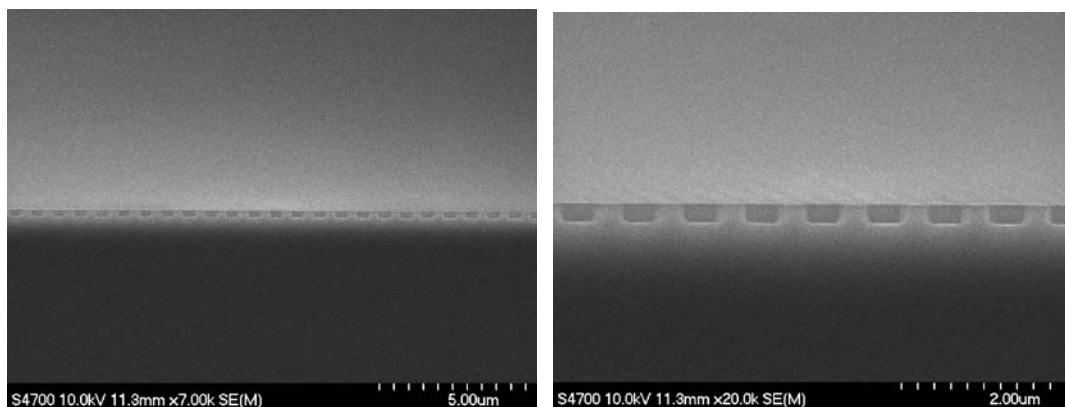

Fig 15. SEM of master pattern (etched silicon wafer) at various magnifications.
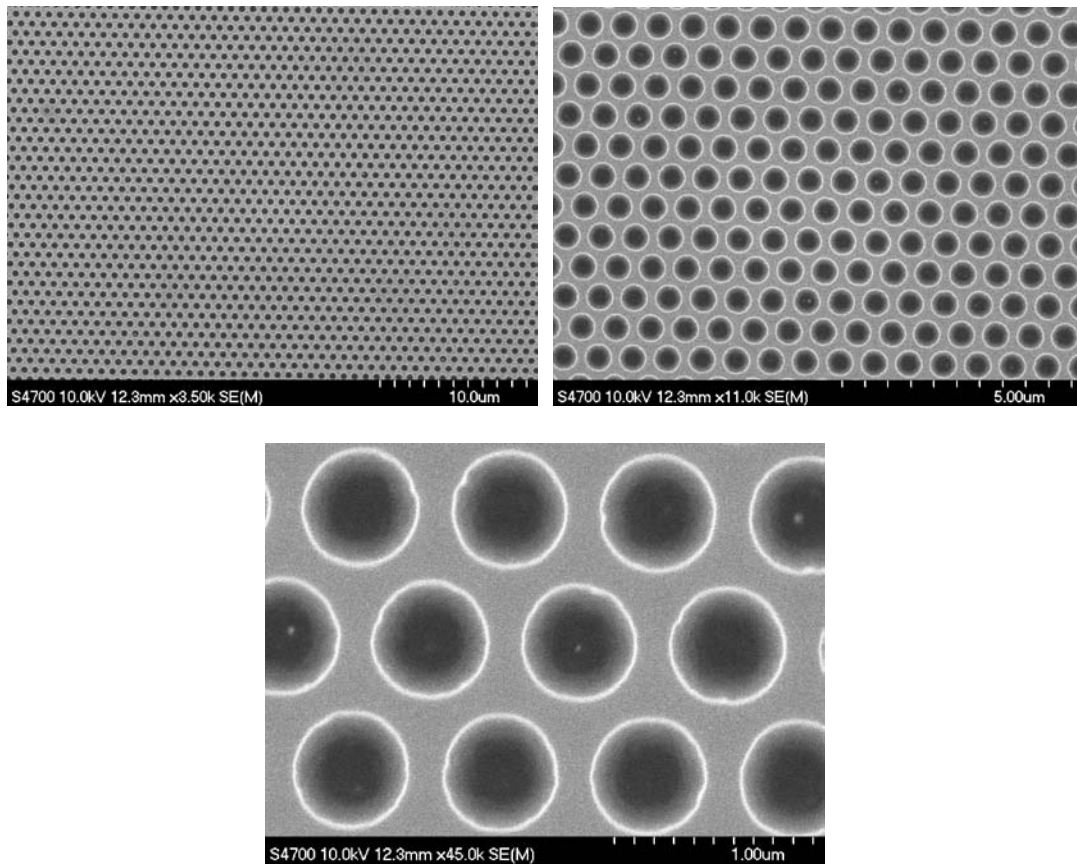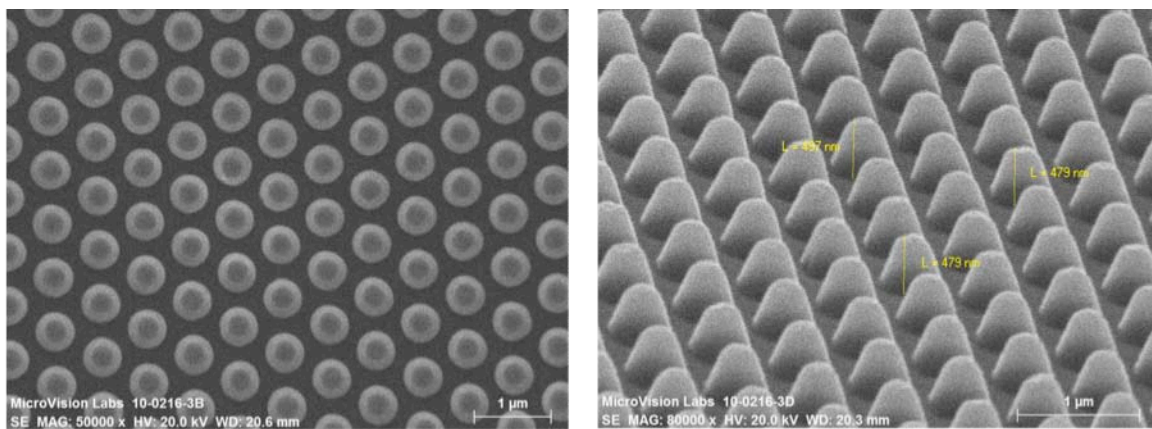
Fig 16. SEMs of etched silicon master pattern (cups). Top three images are normal incidence view of surface of wafer after etching at various magnifications (holes are 750 nm dia). Bottom row shows cross-section of same holes at 2 magnifications.

SEM @ normal incidence

SEM @ 60 degree tilt

Fig 17. Normal incidence SEMs of PBG polymer bump structures

After PBG pattern was imprinted into polymer layer on flexible substrate, the film was placed into a vacuum chamber and outgassed prior to Si deposition in order to stabilize the polymer to resist the PE-CVD temperature (see Fig 18). The outgassing procedure that was developed was as follows:
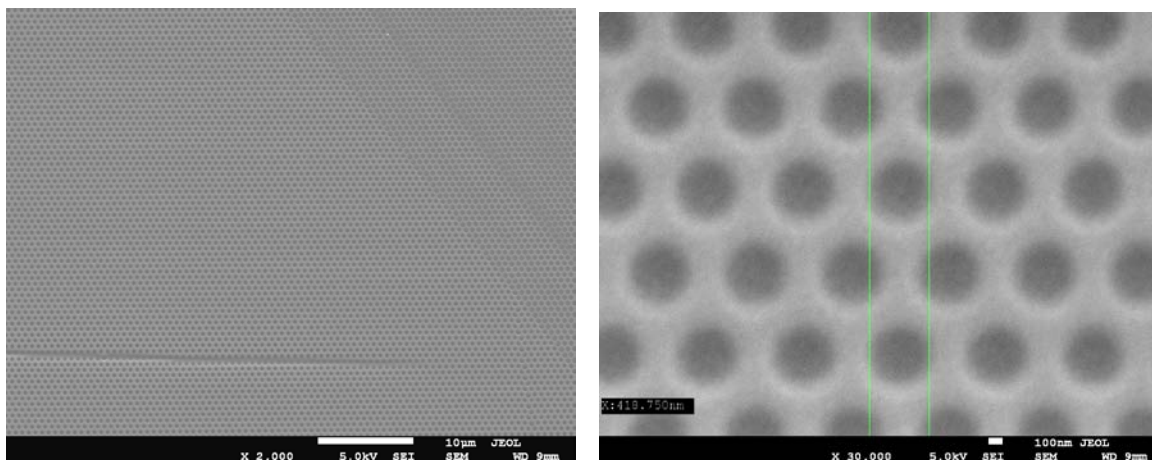

Fig 18. **SEMs of imprint polymer after outgassing tests (hole pattern shown). Outgassing was carried out prior to vacuum heating to improve temperature resistance of imprint polymer.**

1. Samples were loaded individually through a load lock into a vacuum chamber preheated to 300°C and pumped down to better than 6×10^{-7} Torr.

2. Transferring a sample into the main vacuum chamber caused the temperature to drop by about 100°C, which was then recovered within less than 2 min.

3. Each sample was annealed for 2 hours in the vacuum better than 4×10^{-7} Torr.

4. Vacuum changes happening during this time were recorded.

5. After the test, each sample was inspected by SEM. A control sample (obtained from the same sheet, i.e. prepared simultaneously with the test sample), which was not annealed, was inspected as well.
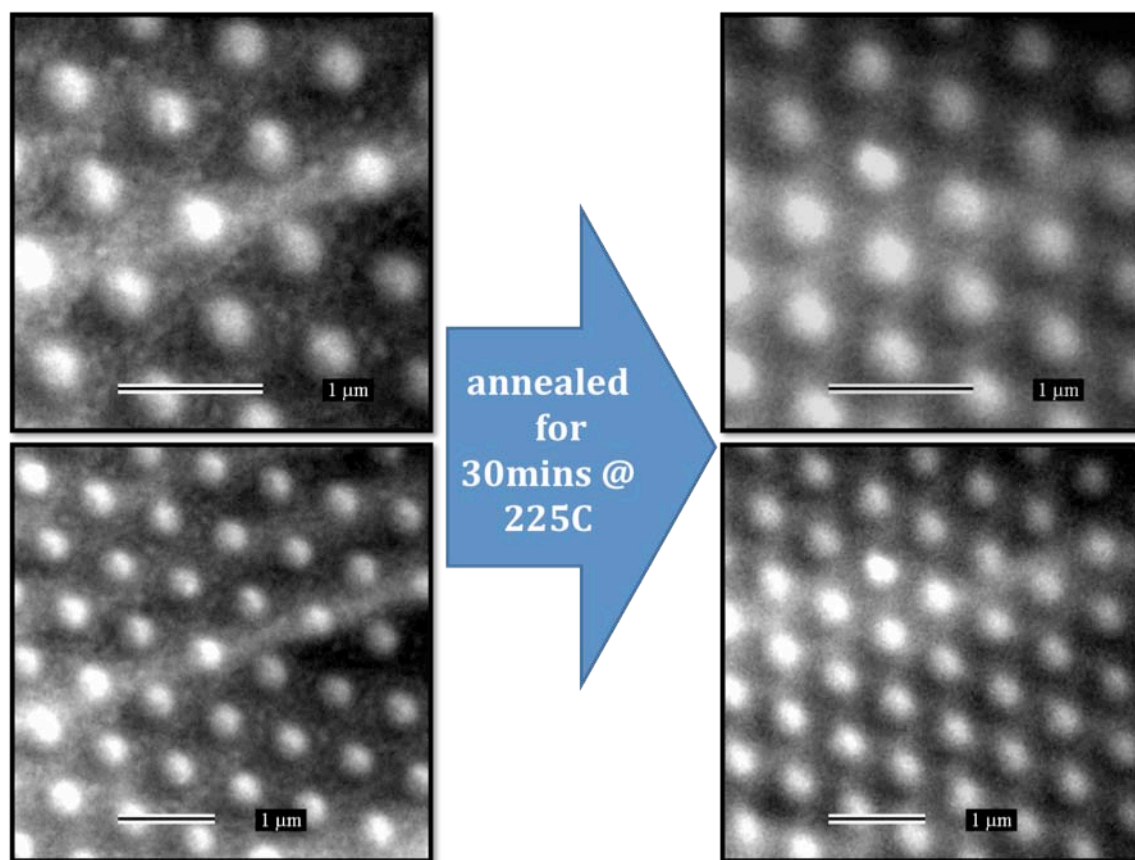
Fig 19. Evaluation of nanoimprinted polymer materials after vacuum annealing at elevated temperatures (stainless steel reference substrate used to eliminate substrate thermal effects)

Figs. 18 & 19, showing the imprinted polymer layer before and after vacuum annealing (225C for 30 min) indicate that the pattern is not deformed by high temperature annealing. Fig. 20 shows photographs of the imprinted polymer substrates illuminated so as to show diffractive separation of light at different angles of incidence due to the periodicity of the nanopattern.
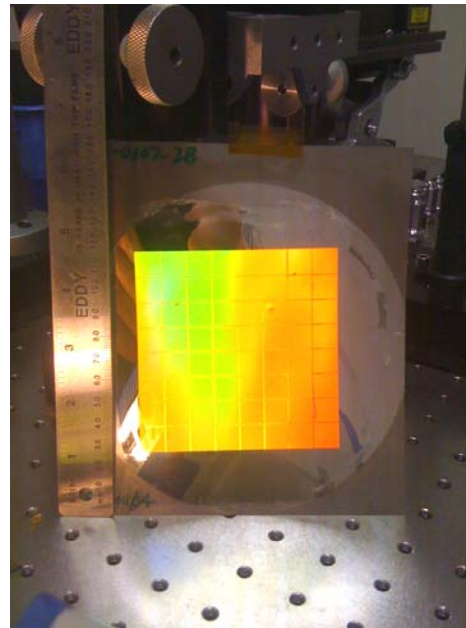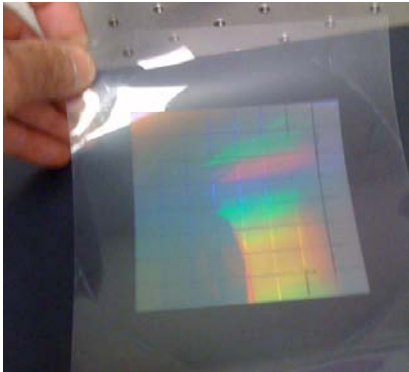
Fig 20. Transparent polymeric substrate with nano-imprinted PBG layer (left: 5 mil thick PEN) and after metallization (right).

Fabrication of Solar Cells

Multiple single junction cells were made during Q2 and sent to Dr. H. Ullal (late April 2010) and verified in May by NREL as having efficiency >4.5 %. These met the requirements of **Deliverable #2**, and the NREL test results are reproduced in Appendix A at the end of this report.

Program Tasks also included efforts to "improve PBG-patterned substrate with…improved temperature resistance." Given the thermal limitations of the cost-effective substrates (PET & PEN), other substrates are being investigated to meet this requirement. By modifying our process for forming PBG patterns, we have been successful in incorporating them onto polyimide plastic films as well as inexpensive grade stainless steel foil (in gauges from ~12μm to 1.25mm). Such substrates will allow much higher CVD deposition temperatures and improved device performance. A photo of the PBG pattern on a 150mm x 150mm foil substrate is given in Fig. 21.

By Q3, the nanoimprinting of the photonic substrate had been improved to the point that the desired pattern can routinely and accurately be reproduced on flexible polymeric (PEN or polyimide) substrates. The work then focused on improving throughput to enable sufficient substrates to be made to support the development of the tandem cells, and this was successfully accomplished during Q3. The resulting efficiency was higher than the target (7.5%), albeit on an area that is smaller. But it demonstrates that we can indeed achieve high efficiencies by using the photonic reflector concept on a flexible substrate.

4   REVIEW OF MILESTONES & DELIVERABLES

The Milestones & Deliverables as set out in the SOW for Q1 were as follows:

Milestone 1 – Completion of PBG Structure Design*	Month 1	2/28/10
Milestone 2 – Completion of NIL Tooling	Month 2	3/28/10
Milestone 3 – PGB Pattern on Polymer Substrates	Month 2	3/28/10
Milestone 4 – Optical Measurement PBG Pattern	Month 2	3/28/10
1st Quarterly Progress Report	Month 3	4/28/10

*Baseline Deliverable

All Milestones for Q1 were achieved on schedule (or slightly early).

The SOW Milestones & Deliverables for Q2 were as follows:

Milestone 5 - Demonstrate Solar Cell with Single Junction 4.5% Conversion Efficiency with a total area of 0.25 cm^2	Month 6	+6 mo
2nd Quarterly Progress Report	Month 6	+6 mo

All Milestones for Q2 were completed on time, and Task #5 was accomplished early.

The Milestones & Deliverables as set out in the SOW for Q3 are as follows:

3rd Quarterly Progress Report	Month 9	+9 mo
Milestone 6 - Improved PBG Substrate	Month 9	10/28/10

The Milestone for Q3 (#6) was completed during this reporting period.

The Milestone & Deliverable for Q4 was as follows:

Milestone 7 - Demonstrate Tandem Solar Cells with 7.5% Conversion Efficiency with a total are of 0.25cm^2	Month 12	1/28/11

The **Final Milestone** (#7) and **Final Deliverable** was completed on time during the final reporting period. Results from NREL testing are given in Appendix B.

5   SUMMARY OF RESULTS

In summary, subcontractor has delivered on all the Goals, Milestones & Deliverables of the research project. As described above, LWP/ISU has fabricated novel photonic structures on plastic substrates, fabricated tandem junction a-Si/nano Si solar cells on these flexible substrates, and has demonstrated that the use of such plastic substrates increases the short-circuit current generated in the solar cells significantly. Total-area, conversion efficiency of 4.62% for single junction a-Si solar cell has been demonstrated, and for the tandem junction a-Si/nano-Si solar cell total-area conversion efficiency achieved was 7.6% on plastic substrates. Two scientific papers were published as a result of this research effort.

APPENDIX A

Statement of Completion of Delivery #2

Subcontract No. NEU-0-99010-05
Prime Contract No. DE-AC36-08GO28308

NREL Report Summary:

◆ NREL

Photovoltaic Cell Data Compilation

Calibration Conducted For:
Harin Ullal
NREL
(for Iowa State University)

PV Testing Group   National Renewable Energy Laboratory
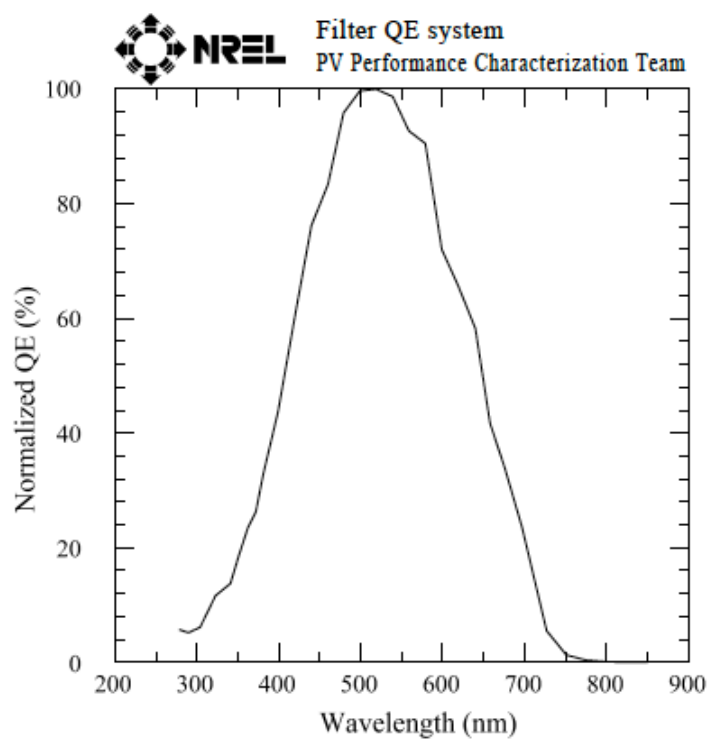Photovoltaic Cell Data Compilation   5/17/2010

Contents

Cell ID	Graph type	Filename	Page
2/13365-B2	FQE	FQE 100511-100548	3
2/13365-B2	X25 LIV	X25 LIV 100517-090341	4
2/13365-B2	X25 DIV	X25 DIV 100517-090951	5
2/13370-B3	FQE	FQE 100511-094904	6

Iowa State University
a-Si Cell

Device ID: 2/13365-B2
May 11, 2010 10:05

Device Temperature: 24.6 ± 0.1°C
Device Area: 0.267 cm^2

Filter QE system
PV Performance Characterization Team

Voltage bias: 0.000E+0 V
Light bias current: 0.4 mA
Light Biased area: 0.27 cm^2
Light bias current density: 2 mA/cm^2

Cal: FQE pyro - ref cell cal 100511-08533

20

Iowa State University

a-Si Cell

Device ID: 2/13365-B2   Device Temperature: 24.7 ± 0.5 °C

May 17, 2010 09:03   Device Area: 0.2667 cm^2

Spectrum: ASTM G173 global   Irradiance: 1000.0 W/m^2

NREL   X25 IV System

PV Performance Characterization Team
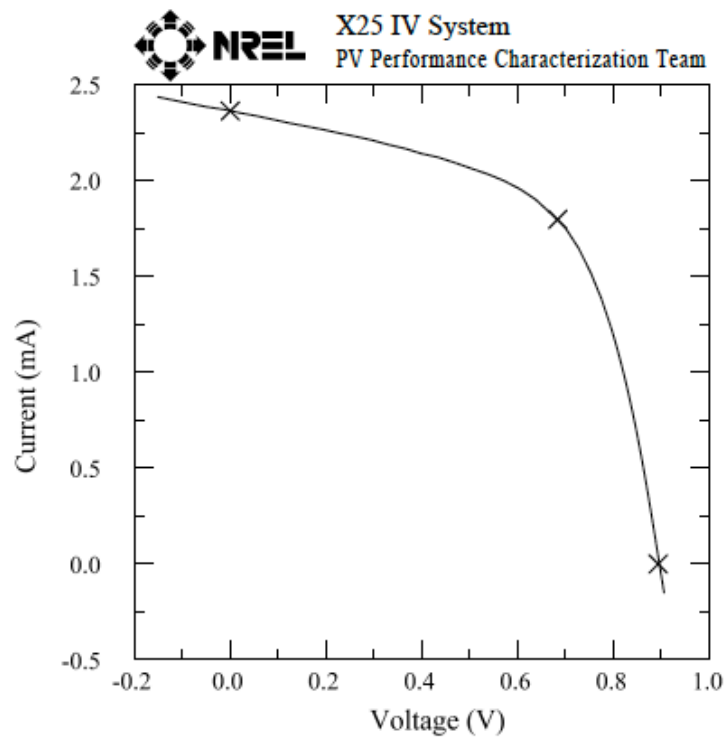
V_{oc} = 0.8942 V I_{max} = 1.7995 mA

I_{sc} = 2.3652 mA V_{max} = 0.6840 V

J_{sc} = 8.8685 mA/cm^2 P_{max} = 1.2308 mW

Fill Factor = 58.19 %   Efficiency = 4.62 %

Storage state

21

Iowa State University
a-Si Cell

Device ID: 2/13365-B2

May 17, 2010 09:09

Device Temperature: 24.7 ± 0.5 °C

Device Area: 0.2667 cm^2
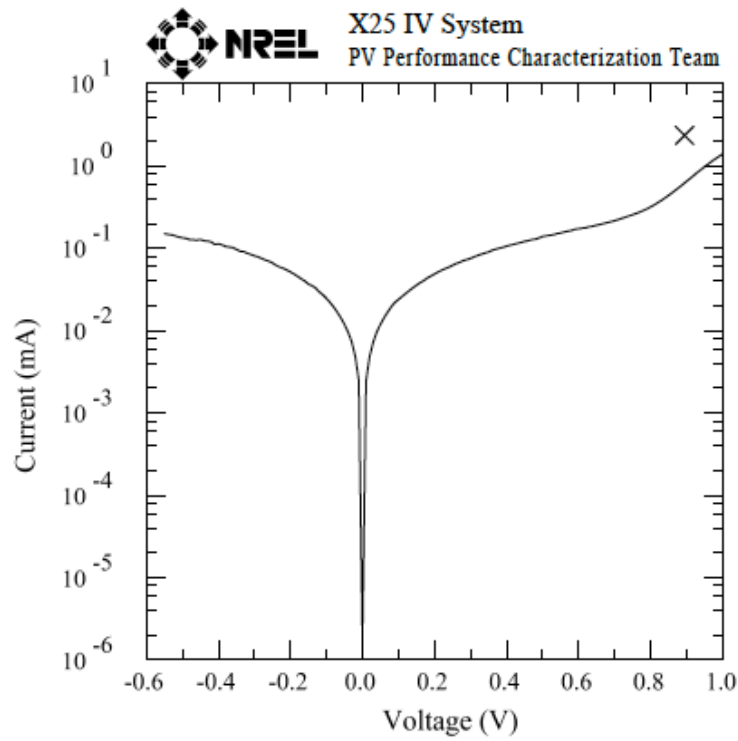
R @ max V = 1.109E+2 Ohms

R @ min V = 3.487E+3 Ohms

Ref V_{oc} = 0.8942 V

Ref I_{sc} = 2.3652 mA

Iowa State University
a-Si Cell

Device ID: 2/13370-B3

Device Temperature: 24.6 ± 0.4°C

May 11, 2010 09:49

Device Area: 0.266 cm^2
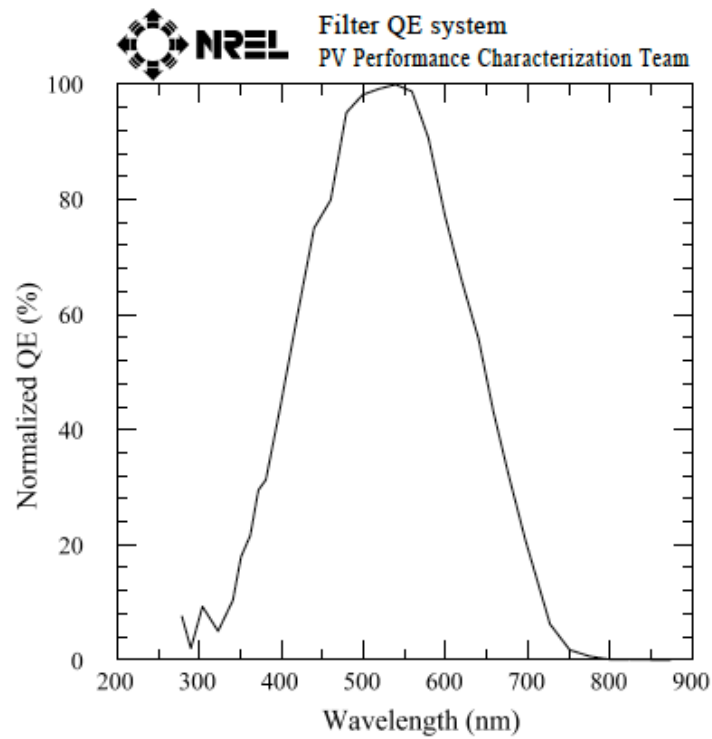
Voltage bias: 0.000E+0 V

Cal: FQE pyro - ref cell cal 100511-08533

Light bias current: 0.5 mA

Light Biased area: 0.27 cm^2

Light bias current density: 2 mA/cm^2

23

APPENDIX B

I-V and QE Curves
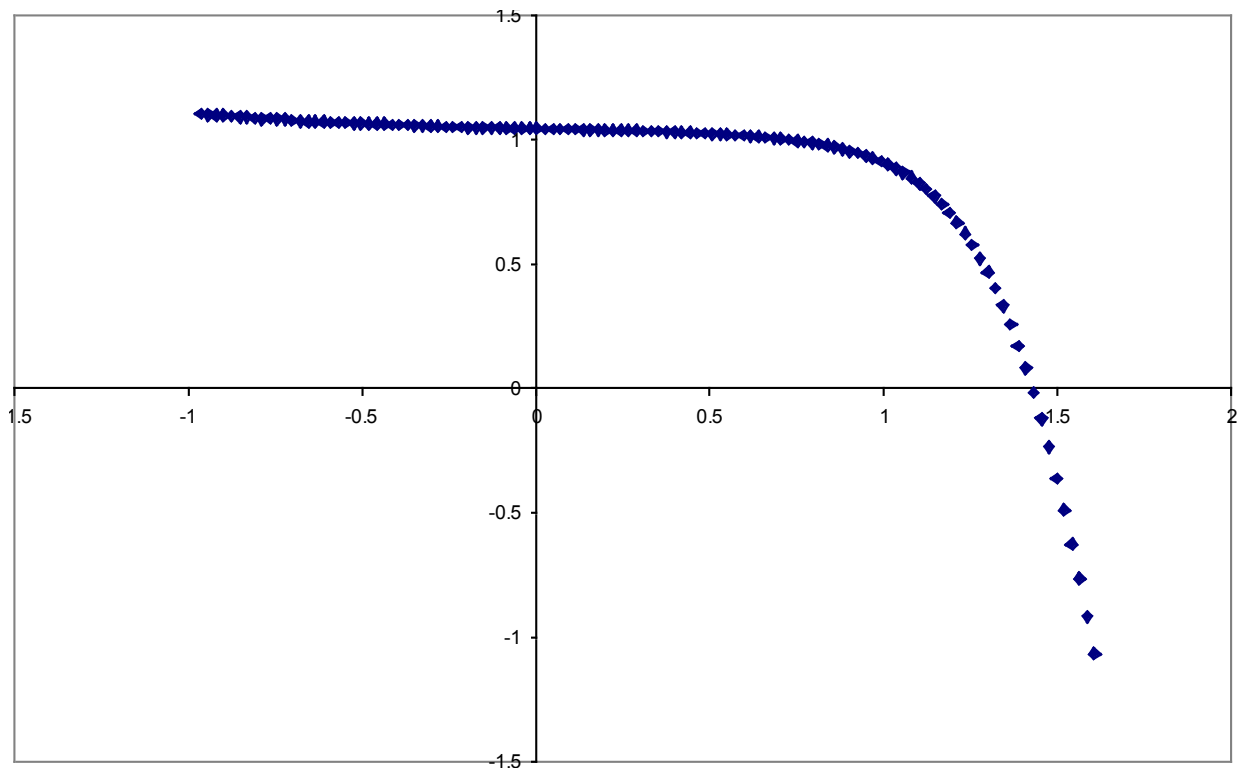
Fig. 1 I-V curve with J~9.8 mA/cm^2, Voc~1.40 V and FF ~0.62, for an efficiency of ~8.5% on an area of 0.12cm^2.
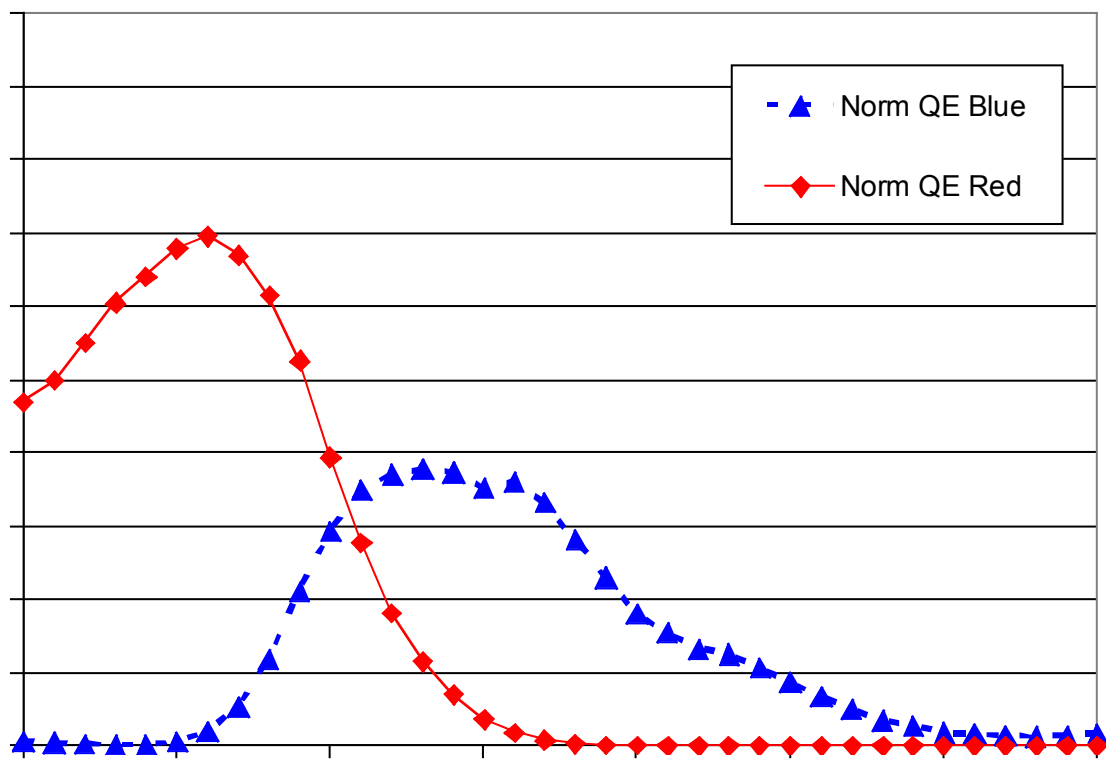
Fig. 2 QE of the components of tandem cell measured using blue and red bias.

APPENDIX C

Statement of Completion of Final Deliverable

Subcontract No. NEU-0-99010-05
Prime Contract No. DE-AC36-08GO28308

NREL

Photovoltaic Cell Data Compilation

Calibration Conducted For:
Harin Ullal
NREL
(for Iowa State University)

Comments
These cells could not be cooled adequately, so there is a difference between the initial "fast Voc" and the Voc of the LIV curve.

Data Collected By:
National Renewable Energy Laboratory
Solar Cell/Module Performance Group
1617 Cole Blvd.
Golden, CO 80401

Contact:
Paul Ciszek
(303) 384-6647
Paul.Ciszek@nrel.gov

Contents

27

Iowa State University
a-Si/multi-Si Cell

Device ID: 2-14557

Feb 09, 2011 14:51

Spectrum: ASTM G173 global

Device Temperature: 24.5 ± 0.5 °C

Device Area: 0.2500 cm^2

Irradiance: 1000.0 W/m^2

X25 IV System

PV Performance Characterization Team

V_{oc} = 1.3498 V

I_{sc} = 2.0235 mA

J_{sc} = 8.0945 mA/cm^2

Fill Factor = 63.58 %
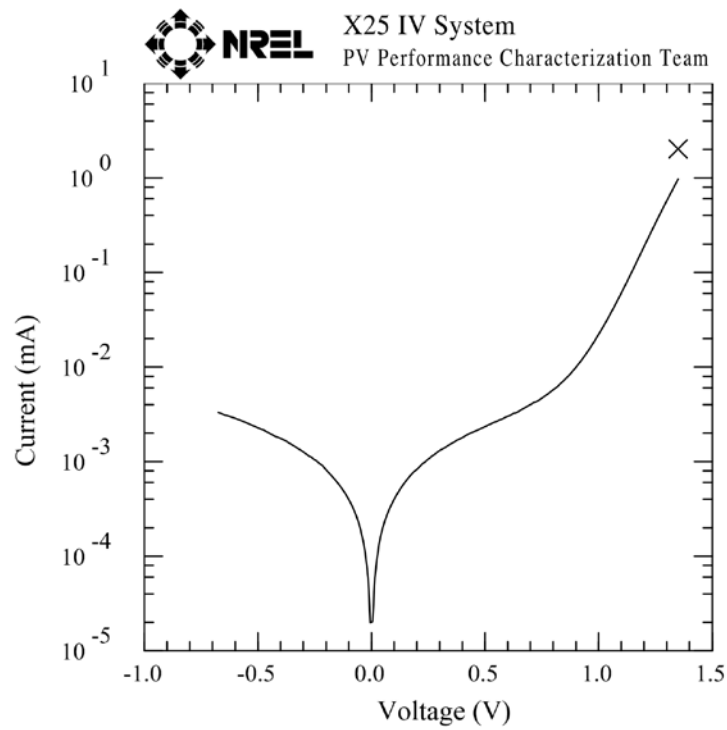
I_{max} = 1.6956 mA

V_{max} = 1.0241 V

P_{max} = 1.7366 mW

Efficiency = 6.95 %

With fan for cooling

Iowa State University
a-Si/multi-Si Cell

Device ID: 2-14557

Device Temperature: 24.5 ± 0.5 °C

Feb 09, 2011 14:54

Device Area: 0.2500 cm^2

R @ max V = 1.082E+2 Ohms

Ref V_{oc} = 1.3498 V

R @ min V = 1.325E+5 Ohms

Ref I_{sc} = 2.0235 mA

With fan for cooling

29

Iowa State University
a-Si/multi-Si

Sample: 2-14563

Temperature = 25.0 ± 2°C

Feb 03, 2011 11:46

Device Area = 0.2500 cm^2

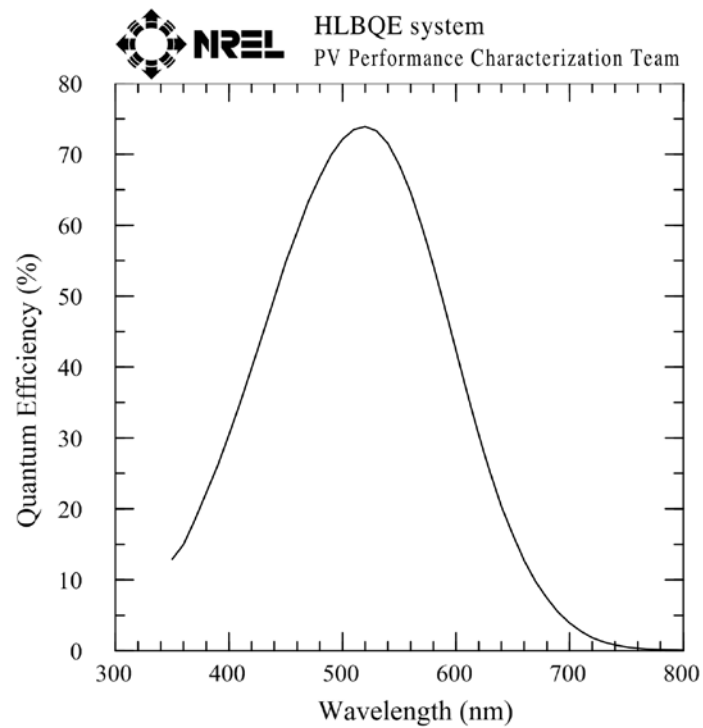HLBQE system
PV Performance Characterization Team
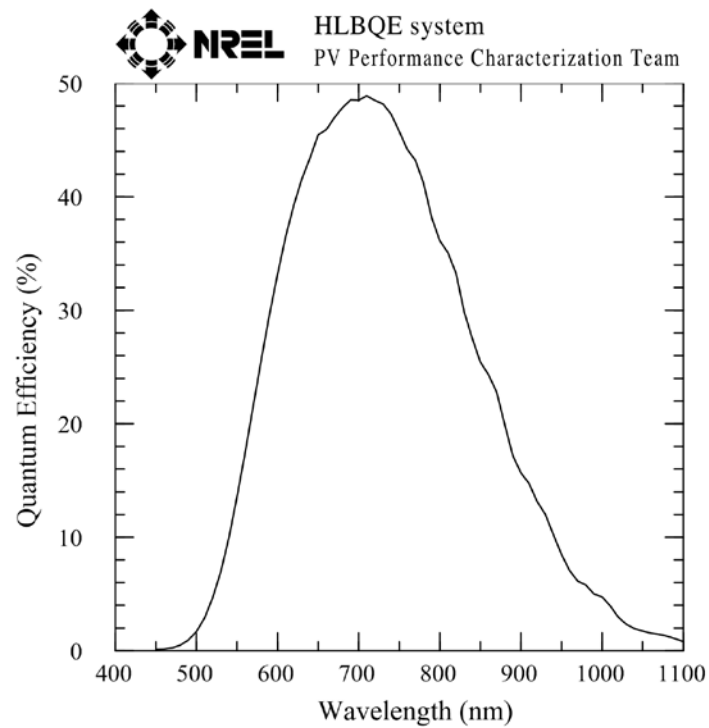
zero voltage bias

Light Bias = 0.190 mA into 0.25 cm^2

Bottom using 2 bias lights each with 600SWP +KG5

Iowa State University
a-Si/multi-Si

Sample: 2-14563

Temperature = 25.0 ± 2°C

Feb 03, 2011 13:25

Device Area = 0.2500 cm^2

HLBQE system
PV Performance Characterization Team

zero voltage bias

Light Bias = 0.0340 mA into 0.25 cm^2

Top using 2 bias lights each with 700LWP filter

31

Iowa State University
a-Si/multi-Si Cell

Device ID: 2-14563
Feb 09, 2011 14:23
Spectrum: ASTM G173 global

Device Temperature: 24.6 ± 0.5 °C
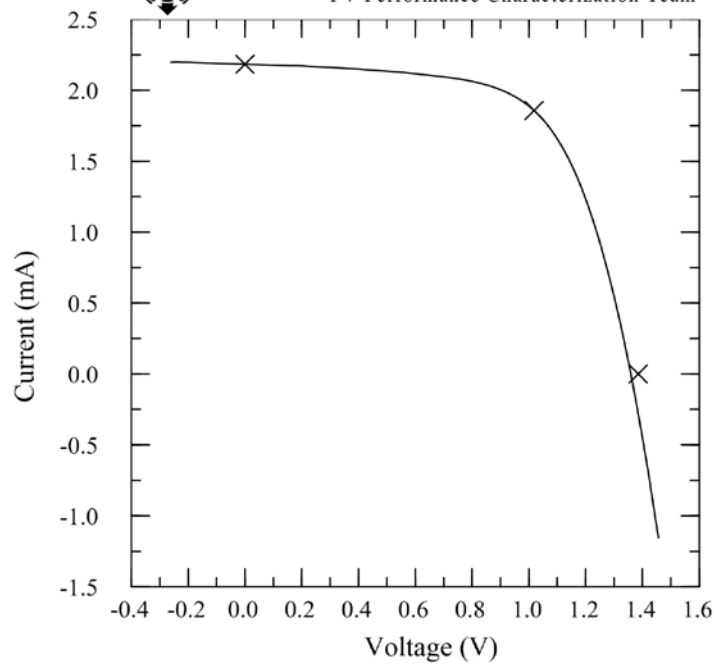Device Area: 0.2500 cm^2
Irradiance: 1000.0 W/m^2

NREL

X25 IV System
PV Performance Characterization Team

V_{oc} = 1.3856 V
I_{sc} = 2.1830 mA
J_{sc} = 8.7322 mA/cm^2
Fill Factor = 62.53 %

I_{max} = 1.8571 mA
V_{max} = 1.0186 V
P_{max} = 1.8916 mW
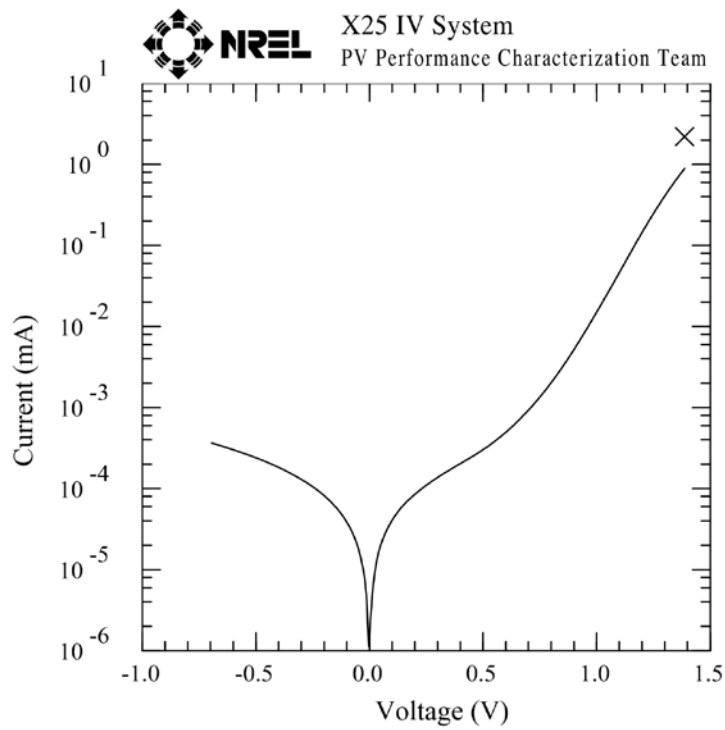Efficiency = 7.57 %

With fan for cooling

Iowa State University
a-Si/multi-Si Cell

Device ID: 2-14563   Device Temperature: 24.8 ± 0.5 °C
Feb 09, 2011 14:17   Device Area: 0.2500 cm^2

X25 IV System
PV Performance Characterization Team

R @ max V = 1.440E+2 Ohms   Ref V_{oc} = 1.3869 V
R @ min V = 1.361E+6 Ohms   Ref I_{sc} = 2.1901 mA

33

Iowa State University
a-Si/multi-Si Cell

Device ID: 2-14573

Feb 09, 2011 14:37

Spectrum: ASTM G173 global

Device Temperature: 24.5 ± 0.5 °C

Device Area: 0.2458 cm^2

Irradiance: 1000.0 W/m^2

X25 IV System

PV Performance Characterization Team

NREL

V_{oc} = 1.3782 V

I_{sc} = 2.4505 mA

J_{sc} = 9.9695 mA/cm^2

Fill Factor = 55.32 %

I_{max} = 2.0054 mA

V_{max} = 0.9316 V

P_{max} = 1.8684 mW

Efficiency = 7.60 %

34

Iowa State University
a-Si/multi-Si Cell

Device ID: 2-14573

Feb 09, 2011 14:41

Device Temperature: 24.5 ± 0.5 °C

Device Area: 0.2458 cm^2

X25 IV System
PV Performance Characterization Team

R @ max V = 1.985E+2 Ohms

R @ min V = 2.408E+6 Ohms

2nd run

35

REFERENCES

1. See www.solarbuzz.com
2. http://solarbuzz.com/facts-and-figures/retail-price-environment/solar-electricity-prices
3. http://www.uni-solar.com/
4. Y. Nakata, Proceedings of 2011 IEEE Technology Management Conference (ITMC) (2011)
5. http://www.solarpanelbuzz.com/solarpanels.kaneka.html
6. B. Yan Baojie; G. Yue, L. Sivec, J. yang and S. Guha, Appl. Phys. Lett. 99, Article Number: 113512 (2011)
7. A. V. Shah, J. Meier, E. Vallat-Sauvain, N. Wyrsch, U. Kroll, C. Droz and U. Graf, Solar Energy Materials and Solar   cells, 78, *469* (2003)
8. J. Müller, O. Kluth, S. Wieder, H. Siekmann, G. Schöpe, W. Reetz, O. Vetterl, D. Lundszien, A. Lambertz, F. Finger, B. Rech and H. Wagner, Solar Energy Materials and Solar Cells, 66, 275(2001)
9. B. Yan, G. Yue, L. Sivec, J. yang, S. Guha, Proc. Of Conference: SPIE Conference On Thin Film Solar Technology II Location: San Diego, CA (2010)
10. Rana Biswas, Dayu Zhou, Proc. Of MRS, 989- A03-02 (2007)
11. D. Y. Zhou and R. Biswas, J. Appl. Phys. 103, May 2008.
12. B. Curtin,R. Biswas, V. L. Dalal et al, Appl. Phys. Lett., 95, 2009.
13. Biswas Rana; Xu Chun; Optics Express, 19, A664-A672 (2011)
14. J. J. Cowan, *Aztec surface-relief volume diffractive structure*, OSA A, Vol. 7, Issue 8, pp. 1529-1544 (1990)
15. A. Vaseashta, V. L. Dalal, A. Greenwald and W. Halverson, Proc. of 18th. IEEE Photovolt. Spec. Conf., 847(1985)
16. V. L. Dalal, M. Leonard, J. F. Booker and A. Vaseashta, Proc. of 18th. IEEE Photovolt. Spec. Conf., 847(1985)
17. B. J. Yan, G. Z. Yue, Yang J and S. Guha, Appl. Phys. Lett. 85,1955 (2004)
18. S. Pattnaik, N. Chakravarty, D. Slafer, R. Biswas and V. L. Dalal, Paper presented at 2011 MRS Conference in San Francisco, Symp. A (2011)-under print.
19. S. Pattnaik, V. Dalal, D. Slafer and Jin Ji, Proc. of IEEE PVSC (2010)
20. Bhattacharya Joydeep; Chakravarty Nayan; Pattnaik Sambit; Biswas, R; Dalal V.L. Source: Appl. Phys. Lett. 99, Article # 131114 (2011)